Prediction of High-Energy Electron Flux at Geosynchronous Orbit using a Neural Network Technique

Ami Iwabu
Kyushu Institute of Technology, 1-1 Sensui-cho, Tobata-ku, Kitakyushu-shi,Fukuoka, 804-8550, Japan

Kentaro Kitamura
Kyushu Institute of Technology, 1-1 Sensui-cho, Tobata-ku, Kitakyushu-shi,Fukuoka, 804-8550, Japan
E-mail: iwabu.ami593@mail.kyutech.jp, kitamura.kentaro375@mail.kyutech.jp
https://www.kyutech.ac.jp

Abstract

The radiation belt, where the high-energy particles are predominant in near earth space from the low earth orbit (LEO) to the geostationary orbit (GEO), sometimes causes satellite malfunction. Therefore, the objective of this study is to predict the high-energy electron flux at GEO with the energy above 2 MeV after 24 hours with higher accuracy for the safety satellite operation in terms of the space weather science. In this study the various kinds of solar wind data from satellite observations and ground geomagnetic observation data in 1999 were used for the Recurrent Neural Network (RNN). Prediction results were evaluated by the prediction efficiency, which is derived from both predicted and actual variation data. As a result, the prediction using combined data of solar wind and geomagnetic data shows highest prediction efficiency of 0.72.

Keywords: Neural network, Spacecraft, High-energy electron flux

1. Introduction

The region in space where high-energy particles are concentrated is called the radiation belt, and the electrons that exist there are called radiation belt electrons. The radiation belts consist of the inner and outer belts. In particular, the outer belt sometimes extends into geostationary orbit, where many satellites are operated [1], [2], [3]. High-energy electrons with energies above MeV are known to cause satellite malfunctions and failures [4], [5].

So far, several studies have been conducted to predict fluctuations in high-energy electron flux by using only ground-based observation data as input parameters or combining ground-based observation data with solar wind data observed in space [6]. Fukada *et al.* [7] used only ground-based AE index and D_{st} index data during magnetic storms as input data and made predictions using a neural network. In their study, predictions were made from 2 to 12 hours later, and the prediction efficiency was as high as 0.71. However, since only the case of magnetic storms was used as training data, it was not practical because it could not predict the starting point where the high-energy electron flux fluctuates significantly. Nakamura *et al.* [8] used seven solar wind data as input data: V_{sw}: solar wind velocity, Bx: solar direction component of solar wind magnetic field data, B_z: north-south component of solar wind magnetic field data, E: electron flux with energy above 2 [MeV], and AE index, D_{st} index, and UT: universal standard time as ground observation data, The same neural network was used to make predictions. In their study, data from 1999 to 2006 were used to predict the energetic electron flux 24 hours later by combining space-based and ground-based data, and the prediction efficiency was 0.61. There is room to further improve this prediction efficiency by the number of input data and the way they are combined.

In this study, with the aim of further improving the prediction accuracy, we use various combinations of ground-based observation data and solar wind data as input data to predict the energetic electron flux over the next 24 hours. The results are also evaluated using prediction efficiency (PE).

2. Dataset

In this study, solar wind velocity (V_{sw}), north-south component of the solar wind magnetic field (B_z), and high-energy (>2 MeV) electron flux (E), which are solar wind data, and AE index, AU index, AL index, D_{st} index, and Universal Time (UT), which are ground-based observation data, as input parameters. AE, AU and AL indices are used as a proxy of the Auroral activity, and

Dst index apparently represents the intensity of the Magnetic storms. We also used Akasofu ε parameter calculated by Eq. (1) [9], which efficiently represent a total energy transported from the solar wind into magnetosphere. V_{sw} and B_z were obtained from the solar wind probe ACE, which was acquired from Omni Web, and E was obtained from the geostationary satellite GOES10, which was acquired from the Space Weather Prediction Center (NOAA) of the U.S. National Oceanic and Atmospheric Administration. The AE, AU and AL indices, and D_{st} index, which are ground-based observation data, were obtained from the Kyoto University Geomagnetic World Data Analysis Center.

In this study, one year of data in 1999 was used, of which 80% was for training data and 20% was for test data. The respective parameters are shown in Fig. 2-1.

$$\text{Akasofu } \varepsilon = V_{sw} \times |B|^2 \times f(t) \times (7Re)^2 \qquad (1)$$

Re : Earth radius

B : Solar wind magnetic field average

where $f(t) = \left\{\sin\left(\frac{t}{2}\right)\right\}^4$, and the value of t is determined by Bz using the following equation.

$$B_z > 0 \quad t = \arctan\left|\frac{B_y}{B_z}\right|$$

$$B_z < 0 \quad t = \pi - \arctan\left|\frac{B_y}{B_z}\right|$$

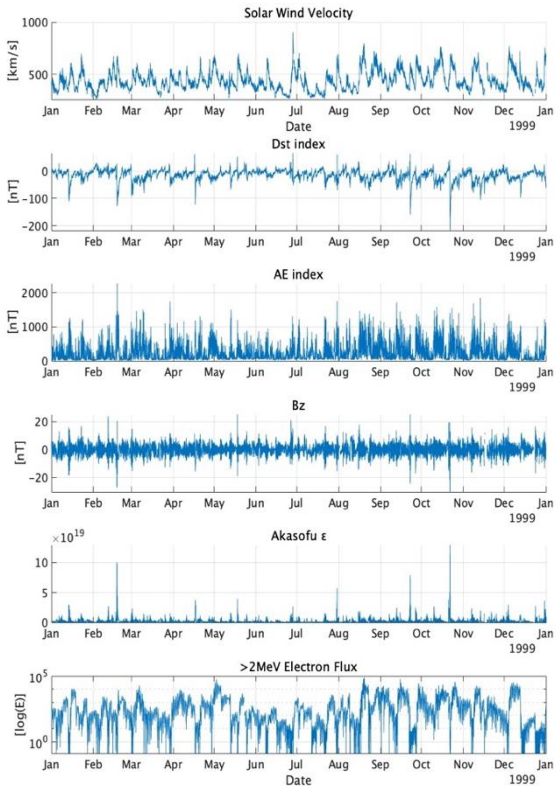

Fig.2-1 Data for each parameter in 1999

Fig.2-1 shows that the temporal variations of solar wind parameters are basically correlated with that of the high-energy electron flux. However, in the short time-scales, the relationship is not necessarily a one-to-one correspondence, but rather a mixture of correlated and uncorrelated portions, indicating a complex relationship among various parameters.

3. Recurrent Neural Network (RNN)

Neural networks are systems that mimic the mechanisms of the human brain in order to perform processes such as recognition, memory, and judgment on a computer. There are two main types of neural networks: supervised learning and unsupervised learning, and supervised learning is used in this study. Supervised learning is a learning method in which an input signal is given and the output signal is repeatedly compared with a teacher signal, and the coupling loadings of each neuron are modified to reduce the error and adapt to a given problem [10].

In this study, a recurrent neural network (RNN) was employed to learn and predict the data. Here, RNN is a neural network that recursively repeats learning in each unit and is suitable for use on continuous data, as shown in Fig.3-1.

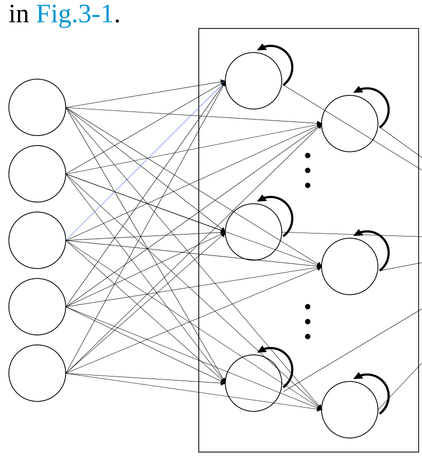

Fig.3-1 Structure of RNN

4. Results

In this study, predictions were made for various combinations of parameters as shown in Table 4-1, and the results were evaluated using the prediction efficiency (PE) shown in Eq. (2),

$$PE = 1 - \frac{MSE}{VAR} \qquad (2)$$

$$MSE = \frac{1}{N}\sum_{i=1}^{N}(f_i - x_i)^2$$

$$VAR = \frac{1}{N}\sum_{i=1}^{N}(x_i - \bar{x})^2$$

$$\bar{x} = \frac{1}{N}\sum_{i=1}^{N} x_i$$

where x_i in each equation is the actual observed value and f_i is the predicted value.

Predictions were made five times for each epoch in each case. The results for each case are shown in Fig.4-1 to Fig.4-5. The horizontal axis is the number of epochs, the vertical axis is PE, and the average value of the five predictions in each epoch is shown as a dot.

Table 4-1 Input data for each forecast

Case 1	V_{sw}, E, B_z, D_{st} index, AE index
Case 2	V_{sw}, E, B_z, D_{st} index, AE index, UT
Case 3	V_{sw}, E, D_{st} index, AEindex, Akasofu ε
Case 4	V_{sw}, E, B_z, D_{st} index, AU index, AL index
Case 5	V_{sw}, E, B_z, D_{st} index, AU index,

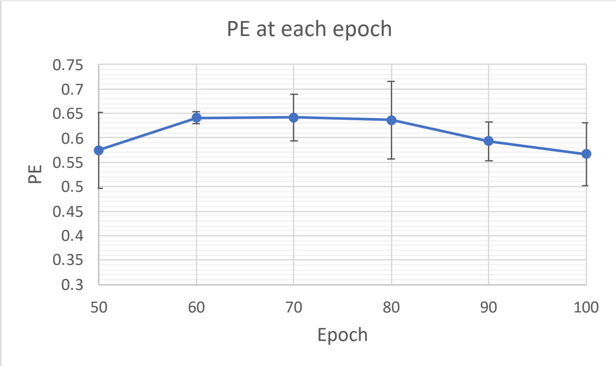

Fig.4-1 PE for case 1

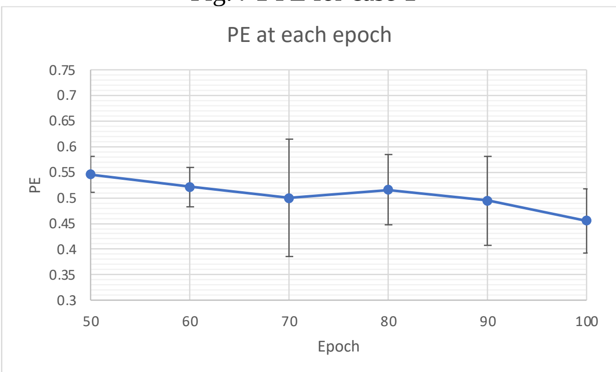

Fig.4-2 PE for case 2

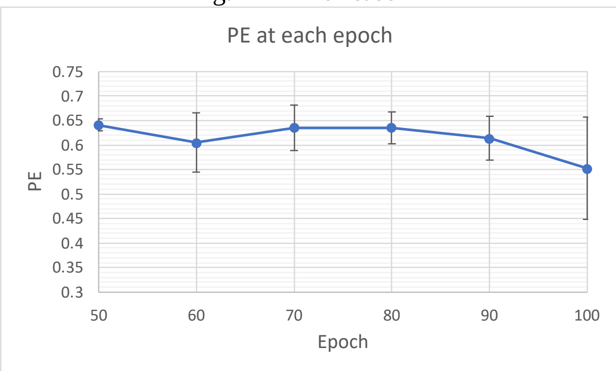

Fig.4-3 PE for case 3

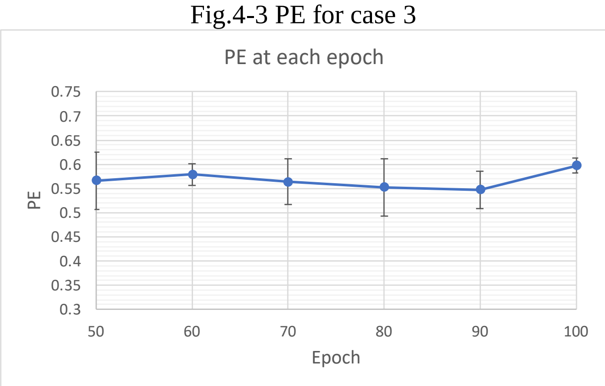

Fig.4-4 PE for case 4

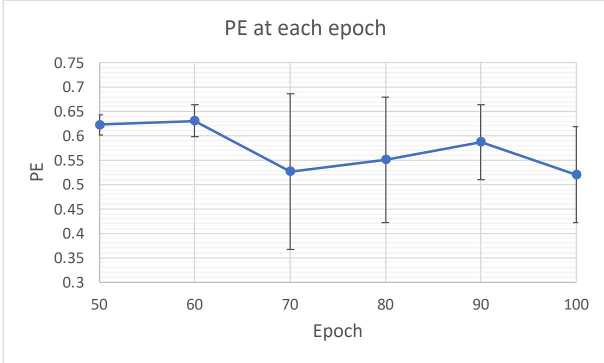

Fig.4-5 PE for case 5

From Fig.4-1 to Fig.4-5, it seems that there is no correlation between the number of epochs and prediction efficiency between epochs 50 and 100.

Next, Table 4-2 shows the average prediction efficiencies obtained from the results for all epochs in each case.

Table 4-2 Comparison of average PE in each case

Case	1	2	3	4	5
Average PE	0.61	0.51	0.61	0.57	0.57

Table 4-2 indicates that Case 2, in which UT (the proxy of the satellite position) was added as input data to Case 1, shows the worst PE, while the case 1 shows the highest PE. On the other hand, Case 3, in which Akasofu ε (the total energy inflow from the solar wind) was added, had the same PE as Case 1.

Case 1 with an epoch number of 70, PE shows the highest value of 0.72. The prediction results for this case are shown in Fig.4-6 and Fig.4-7.

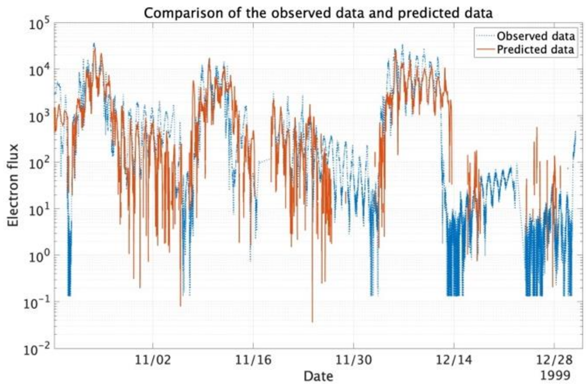

Fig.4-6 Comparison of predicted and observed data at the highest PE

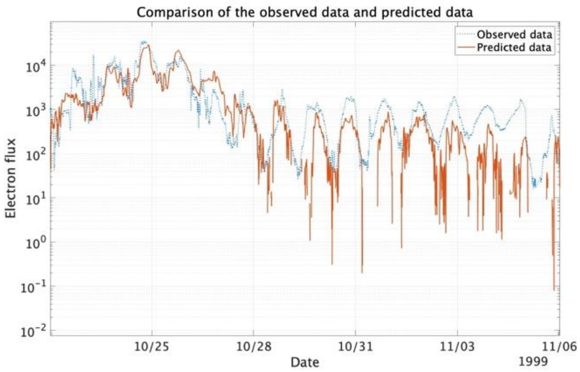

Fig.4-7 Comparison of predicted and observed data at the highest PE

In Fig.4-6 and Fig.4-7 show the comparison of the temporal variations for both predicted and observed high-energy electron flux. The horizontal axis shows the date and the vertical axis shows the energetic electron flux. The blue line shows the actual observed data, and the orange line shows the predicted data. The more the orange line, the predicted data, overlaps the blue line, the observed data, the higher the prediction efficiency and accuracy.

Fig.4-6 shows that the forecast results are largely consistent for large changes. Fig.4-7 shows that the predicted values are lower than the actual observed values in many areas where the value of E is small.

5. Discussion

In Case 2, in which UT (the positional information of the satellite) was added as input data to Case 1, resulted PE is lower than that in Case 1. On the other hand, PE in Case 3 is almost same as that in Case 1, while Case 3 is added one parameter (the Akasofu ε which is the total number of energy inflows from the solar wind) to Case 1 same as Case 2. The difference of the added parameters causes significant difference in consequent result. This suggests that the spatial information might reduce the PE, rather than the increasing of number of input parameters. Especially, using one parameter that include the integrated several information can efficiently improve PE, rather than superposing several parameters that has individual information. On the other hand, the input parameters of solar wind data might have potential to improve the PE compared to that of ground data.

6. Conclusion

In each case, there is no correlation between the number of epochs and the PE, which means that the PE is not dependent on the number of epochs between 50 and 100, and there is no need to set the number of epochs above 100.

From the comparison of the average prediction efficiency for each case, the accuracy of prediction is higher when the parameters to be used as input data have integral information rather than when the number of input data is increased.

From the prediction results, the trend of the change in high-energy electron flux is captured. In addition, in the short time scale, we find that the prediction shows a little underestimation at the time of decreasing of E, but during E has an energy of 10^4 or more (alert level for the satellite malfunction), the prediction is highly accurate. In conclusion, the current result suggests that the RNN method proposed in this study is able to predict the periods considered important for the safe operation of the satellite.

Acknowledgements

The solar wind data obtained by ACE spacecraft and the high-energy electron flux data were provided by the National Oceanic and Atmospheric Administration (NOAA). The D_{st} index, *AE* index *AU* index and *AL* index were provided from the World Data Center (WDC) for Geomagnetism, Kyoto.

References

1. Van Allen, J. A. G. H. Ludwing, E.C. Ray, and C. E. McIlwain (1958), Observations of high intensity radiation by satellites 1958 Alpha and Gamma, Jet Propulsion, 28, 588-592.
2. Van Allen, J. A., and L. A. Frank (1959), Radiation around the Earth to a radial distance of 107,400 km, Nature, 183, 430.
3. Baker DN, McPherron RL, Cayton TE, *et al.* (1990) Linear prediction filter analysis of relativistic electron properties at 6.6 Rea. J Geophys Res 95:15 133-15 140.
4. Lohmeyer, W. Q., and K. Cahoy (2013), Space weather radiation effects on geostationary satellite solid-state power amplifiers, Space Weather, 11, 476–488, doi:10.1002/swe.20071.
5. Baker, D. N. (2000), The occurrence of operational anomalies in space-craft and their relationship to space weather, IEEE Trans. Plasma Sci.,28(6), 2007–2016, doi:10.1109/27.902228.
6. Koga S, Koshiishi H, Matsumoto H, *et al.* (2006) Prediction of electron flux variations at radiation belt (in Japanese). JAXA-SP-05, p 24.
7. Fukata M, Taguchi S, Okuzawa T, and Obara T (2002) Neural network prediction of relativistic electrons in geosynchronous orbit during the storm recovery phase: effects of recurring. Ann Geophys 20:947-951.
8. Nakamura Y, Kitamura K, Tokunaga M, *et al.* (2009) Prediction of electron flux at Geosynchronous Obit by using the Neural Network (in Japanese). JAXA-SP-09, p 6.
9. Akasofu, S.-I. (1981), Energy coupling between the solar wind and the magnetosphere, Space Sci. Rev., 28, 121.
10. Yoshitomi Y (2002), Neural network (in Japanese), Asakura shoten.

Authors Introduction

Ms. Ami Iwabu

She received her Bachelor’s degree in Engineering in 2023 from the Faculty of Engineering, Kyushu Institute of technology in Japan. She is currently a master student in Kyushu Institute of Technology, Japan

Dr. Kentaro Kitamura

He is a Professor of Kyushu Institute of Technology, and director of Laboratory of Lean Satellite Enterprises and In-orbit Experiments (LaSEINE). He received his BS and MS degrees in science from Kyushu University, in 1996 and 1998, respectively. Then he received his Ph.D. degrees in science (Earth and Planetary Science) from Kyushu University in 2001.